

# Graphene Transistors with Multifunctional Polymer Brushes for Biosensing Applications

Lucas H. Hess, Alina Lyuleeva, Benno M. Blaschke, Matthias Sachsenhauser, Max Seifert, and Jose A. Garrido\*

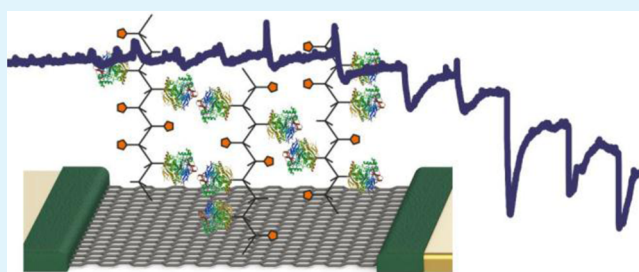
Walter Schottky Institut and Physik-Department, Technische Universität München, Am Coulombwall 4, 85748 Garching, Germany

Frank Deubel<sup>†</sup>

WACKER-Lehrstuhl für Makromolekulare Chemie, Technische Universität München, Lichtenbergstrasse 4, 85748 Garching, Germany

## S Supporting Information

**ABSTRACT:** Exhibiting a combination of exceptional structural and electronic properties, graphene has a great potential for the development of highly sensitive sensors. To date, many challenging chemical, biochemical, and biologic sensing tasks have been realized based on graphene. However, many of these sensors are rather unspecific. To overcome this problem, for instance, the sensor surface can be modified with analyte-specific transducers such as enzymes. One problem associated with the covalent attachment of such biomolecular systems is the introduction of crystal defects that have a deleterious impact on the electronic properties of the sensor. In this work, we present a versatile platform for biosensing applications based on polymer-modified CVD-grown graphene transistors. The functionalization method of graphene presented here allows one to integrate several functional groups within surface-bound polymer brushes without the introduction of additional defects. To demonstrate the potential of this polymer brush functionalization scaffold, we modified solution-gated graphene field-effect transistors with the enzyme acetylcholinesterase and a transducing group, allowing the detection of the neurotransmitter acetylcholine. Taking advantage of the transducing capability of graphene transistors and the versatility of polymer chemistry and enzyme biochemistry, this study presents a novel route for the fabrication of highly sensitive, multipurpose transistor sensors that can find application for a multitude of biologically relevant analytes.



**KEYWORDS:** functionalization, graphene, field-effect transistors, sensors/biosensors, polymers

## INTRODUCTION

Since the isolation of graphene in 2004,<sup>1</sup> it has been recognized that the outstanding properties of this material could provide game-changing benefits in the development of highly sensitive sensors for advanced applications like biosensing or the detection of single molecules.<sup>2,3</sup> Currently, graphene devices have been successfully used in several demanding biosensing applications, such as the detection of cell action potentials,<sup>4,5</sup> protein adsorption,<sup>6</sup> as well as the amperometric detection of different substances.<sup>7,8</sup> Furthermore, the possibility to fabricate microfluidic systems based on graphene transistors facilitates the use of graphene based sensors for practical applications.<sup>9</sup>

To improve the sensitivity and specificity of the sensors, it is of great relevance to modify the rather unspecific sensor's surface with biomolecular systems, in particular enzymes. To obtain stable devices, though, the enzymes should be bound covalently to the sensor surface. However, the covalent attachment of functionalities can induce damage to the graphene lattice<sup>10</sup> and degrade its electronic properties, thus

strongly diminishing the unique competitive advantages of graphene for highly sensitive electronic devices. Recently, a method was presented to graft functional polymers to existing defects in graphene without a negative impact on the crystal quality and a consequent electronic degradation.<sup>11,12</sup> In this way, suitable monomers can be selected to design polymer brushes providing a grafting scaffold for the enzymes doing the biomolecular transduction and, at the same time, introducing additional functional groups that facilitate the detection of the enzyme activity with a transistor.

In this work, we report on a versatile concept for graphene biosensors based on graphene solution-gated field-effect transistors (G-SGFETs) functionalized with multifunctional polymer brushes. The functionalization method reported in this work enables the integration of different functionalities, in our

Received: April 8, 2014

Accepted: May 28, 2014

Published: May 28, 2014

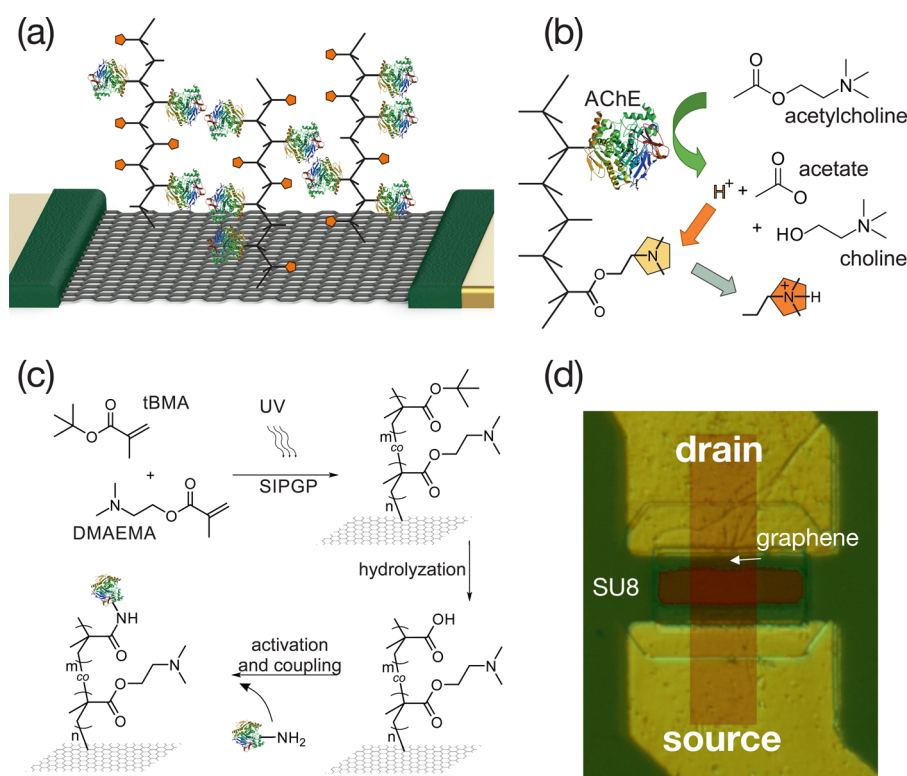


**Figure 1.** (a) Schematic view of an enzyme-functionalized graphene transistor. The graphene sheet is contacted by insulated gold contacts from two sides. The graphene active area is modified with copolymers containing acetylcholinesterase and pH sensitive DMAEMA (orange pentagons) groups. (b) Sensing principle of the transistors. Acetylcholine is hydrolyzed to acetate, choline, and a proton with the help of the enzyme. This proton can react with the dimethylamino groups in the polymer, inducing a fixed charge close to the transistor's surface that results in a charge doping effect. (c) Schematic of the functionalization reactions. DMAEMA and *t*BMA are attached to the surface as copolymer brushes by SIPGP. The *tert*-butyl group is removed by hydrolyzation to expose the carboxyl group, which is then activated by EDC and sulfo-NHS. Finally, the AChE is bound to the activated carboxyl group. (d) Micrograph of a graphene solution-gated transistor.

case the enzyme acetylcholinesterase (AChE) and a transducing pH sensitive group in the polymer brushes, allowing the detection of the neurotransmitter acetylcholine. This neurotransmitter is a very important component of the nervous system of many organisms, including humans, and its detection might provide a better understanding of such systems. Following the transistor fabrication with large-area graphene grown by chemical vapor deposition (CVD) on copper foil,<sup>13,14</sup> functional polymer brushes were grown on the transistors' active area. The functional groups of the polymer brushes allowed both the covalent grafting of the sensing enzyme and the detection of the enzyme's activity. In our case, this detection was done indirectly by using a functional group in the polymer to measure one of the enzymatic reaction products, hydronium, which induces a local change in pH. The pH response of the modified transistors and the activity of the grafted enzyme have been further investigated to gain a better understanding of the sensing experiments.

## EXPERIMENTAL SECTION

**Transistor Fabrication.** The graphene layers were grown by chemical vapor deposition on copper and transferred with a poly(methyl 2-methylpropenoate) (PMMA) film and an iron trichloride etch as described previously.<sup>14</sup> The films were deposited on sapphire substrates prepatterned with Ti/Au leads. By standard photolithographical methods, the graphene was selectively etched by oxygen plasma and a second gold layer was applied. The metal contacts and leads were subsequently covered with chemically stable SU8 photoresist to insulate them from the electrolyte. An optical

micrograph of a G-SGFET ( $10 \times 20 \mu\text{m}^2$ ) is shown in Figure 1d. The transistors were fabricated in arrays of  $8 \times 8$  transistors per sample.

**Surface Functionalization.** The finished transistor structures were functionalized by self-initiated photografting and photopolymerization (SIPGP).<sup>12,11</sup> The samples were carefully heated to  $200^\circ\text{C}$  under vacuum to remove water from the sample surface. Subsequently, they were immersed in freshly distilled and degassed monomer and irradiated with a UV fluorescent lamp. To obtain the desired functionalities, different monomers were used for the preparation of polymers. *N,N*-Dimethylaminoethyl methacrylate (DMAEMA) can provide a well-defined pH sensitivity, whereas *tert*-butyl methacrylate (*t*BMA) incorporates the necessary carboxyl groups for the enzyme immobilization. These monomers were used at a ratio of 1:1.

**Enzyme Immobilization.** The *tert*-butyl protection group of the *t*BMA groups was removed by hydrolyzation with methanesulfonic acid in dichloromethane (1:100). Subsequently, the samples were immersed into a mixture of *N*-hydroxysulfosuccinimide (sulfo-NHS, 100 mM) and 1-ethyl-3-(3-(dimethylamino)propyl)carbodiimide (EDC, 400 mM) in a 2-(*N*-morpholino)ethanesulfonic acid (MES, 100 mM) buffer to activate the carboxyl groups in the polymer brushes for further reaction and peptide bond formation with primary amines.<sup>15</sup> After rinsing with buffer, a solution of acetylcholinesterase from *Electrophorus electricus* (type V-S, 0.2 mg/mL) was applied to the sample surfaces overnight at  $4^\circ\text{C}$ . To prevent competitive grafting of the 2-amino-2-hydroxymethylpropane-1,3-diol (TRIS) buffer contained in the stock enzyme solution, centrifugal filtration was applied. After the enzyme grafting, the remaining activated sites were passivated by a TRIS solution.

**Transistor Measurements.** The transistors were wire-bonded to chip carriers and connected to a system of current–voltage converters and amplifiers as well as a data acquisition setup. This system also provided the biasing voltages applied between the sample contacts and

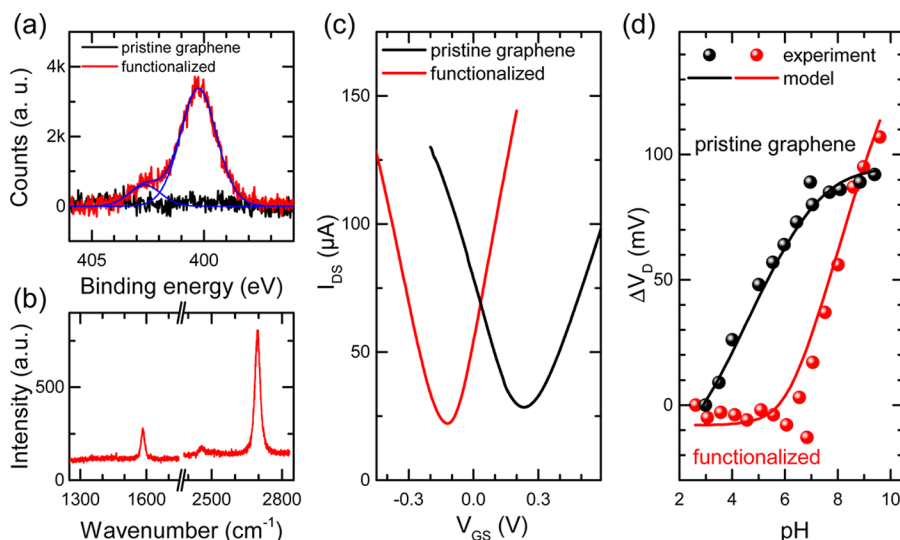


**Figure 2.** (a) High resolution X-ray photoelectron spectra showing the nitrogen 1s core level. After polymerization, the presence of nitrogen from the DMAEMA group can be seen. (b) Raman spectrum of a functionalized sample. The absence of the D peak indicates that no additional defects were induced by the polymerization. (c)  $I_{DS}$  versus  $V_{GS}$  for a pristine graphene transistor and a device modified with polymers containing DMAEMA groups. Both transistors exhibit the typical behavior for graphene with an ambipolar charge transport and a minimum conductivity at the Dirac point  $V_D$ . The position of this point differs for pristine and functionalized transistors. (d) Shift of  $V_D$  with pH for a pristine graphene and a DMAEMA-modified transistor. The pristine graphene transistor saturates at high pH, whereas the functionalized device shows a good sensitivity for pH > 6. The solid lines correspond to the model discussed in the text. Each of the shown data points was obtained by averaging  $V_D$  of several transistors. The observed statistical errors are  $\sim 10$  mV.

a Ag/AgCl reference electrode in the electrolyte, which consisted of 5 mM PBS buffer with a background concentration of 250 mM NaCl for the pH characterization. For probing the acetylcholinesterase's activity, the buffer was changed to 1 mM PBS with 100 mM NaCl and 20 mM  $MgCl_2$ . Small amounts of a highly concentrated acetylcholine solution were added to adjust the desired acetylcholine concentrations.

## RESULTS AND DISCUSSION

Figure 1a shows a schematic of the working principle of the enzyme-functionalized solution-gated graphene transistor employed in this work. A graphene sheet is connected on two sides with gold contacts to apply the biasing voltages to the transistor. To prevent leakage currents, the metal contacts are covered by an insulating, chemically stable resin. On the surface of the transistor, polymer brushes with covalently attached acetylcholinesterase provide specific sensitivity to the neurotransmitter acetylcholine. To detect the activity of the AChE, it is necessary to regard its enzymatic reaction: At the active site of AChE, acetylcholine is hydrolyzed to acetate, choline, and a proton (Figure 1b), which is of crucial importance for this type of sensor. In a next step, the local change in pH due to the released proton changes the charge state of a pH-sensitive functional group of the polymer brush. This charge variation in the vicinity of the graphene induces a small shift of the Fermi level, resulting in a conductivity change that can be detected electrically as discussed below.

Figure 1c shows a schematic depiction of the functionalization processes. First, polymer brushes are grown by self-initiated photografting and photopolymerization (SIPGP)<sup>16,12,11</sup> of methacrylate monomers. In this process, methacrylate monomers are activated by UV illumination and abstract hydrogen atoms from  $sp^3$  carbon defects in the graphene lattice, generating surface radicals on the graphene surface. These activated sites can then start radical polymerization from the surface.<sup>12</sup>

Different monomers were used to obtain the desired functionalities. *tert*-Butyl methacrylate (*t*BMA) was used to create binding sites for the enzymes after saponification to methacrylic acid (MAA). MAA cannot be used directly for the polymerization as it would react with the *N,N*-dimethylaminoethyl methacrylate (DMAEMA) to form ionically cross-linked, nonfunctional polyelectrolyte brushes. As discussed in detail below, the use of DMAEMA enables the introduction of pH-sensitive groups in the working range of the enzyme that allow the detection of the enzyme activity by measuring a byproduct of the enzymatic reaction. In a second step, the carboxyl group of MAA was activated by a standard bioconjugate technique.<sup>15</sup> This activated group then readily binds to primary amines which are present at the enzymes surface. The successful grafting of polymer brushes was confirmed by high resolution X-ray photoelectron spectroscopy of the nitrogen 1s core level. The functionalized samples exhibit a clear presence of nitrogen due to the dimethylamino group in the polymer (Figure 2a). As the dimethyl amino group can be protonated to a positively charged dimethylammonium group, two different peaks are typically observed. The larger peak at 400 eV corresponds to the amino group and the smaller peak at 403 eV to the protonated group.<sup>17</sup>

In summary, the resulting polymer brushes contain both the covalently attached enzyme as well as a transducing element to detect the changes in the local pH induced by the activity of the enzyme.

In Figure 2c, a typical plot of a transistor's drain-source current  $I_{DS}$  versus the applied gate voltage  $V_{GS}$  is shown for a bare and a functionalized device. As described previously,<sup>18</sup> the Fermi level  $E_F$  in graphene can be shifted by applying a gate voltage across the graphene-electrolyte interface, in this case via a Ag/AgCl reference electrode. The shift in  $E_F$  modulates the density of charge carriers in graphene, and eventually their mobility, and therefore results in a change in the conductivity. It can be seen from Figure 2c that the drain-source current of



the graphene transistor reaches a minimum value at a certain gate voltage, called the Dirac point,  $V_D$ . This feature is due to the special band structure of graphene where the valence band and the conduction band meet at the Dirac point; at this bias, the type of majority charge carriers is changed from holes ( $V_{GS} < V_D$ ) to electrons ( $V_{GS} > V_D$ ). Furthermore, a significant shift of the Dirac point is observed for functionalized transistors compared to bare devices, which can be explained by doping due to charges in the polymer brushes. From this shift, a charge density of  $5 \times 10^{12}$  charges/cm<sup>2</sup> can be estimated assuming monovalent charges directly at the surface. The slope of the  $I$ – $V$  curve remains largely unchanged, confirming that the polymerization does not increase the density of defects, in accordance with Raman spectroscopy (Figure 2b) and literature.<sup>11</sup> Over 2 days of experiments, no changes in the  $I$ – $V$  characteristics of the devices could be observed, revealing the stability of the polymer-modified transistors (see Figure S1 in the Supporting Information).

As this type of enzyme-sensing transistor relies on the detection of small changes in pH, the response of the graphene transistors to the solution pH will be discussed in the following. Figure S2 (Supporting Information) shows the  $I$ – $V$  characteristics of a nonfunctionalized graphene solution-gated field-effect transistor while the pH was varied between 3 and 10. While the general shape and the slope of the curve remains almost unchanged, a clear shift of the Dirac point is observed for varying pH. Figure 2d shows the shift of the Dirac point as a function of the pH for bare and functionalized graphene. This will be discussed in terms of charge doping induced by surface groups that can be protonated or deprotonated depending on their acid dissociation constant  $K_a$  and the pH of the electrolyte. At low pH, these groups are mostly protonated; that is, they carry a more positive charge resulting in an increase of the Fermi level with respect to the band structure. As a result, the Dirac point  $V_D$  is expected to shift toward less positive gate voltages, as observed in the experimental data shown in Figure S2. The magnitude of this shift with the pH can be quantified most easily by the determination of the Dirac point  $V_D$ , as shown in Figure 2d. The observed pH dependence of  $V_D$  can be described using the following model. Based on the definition of the acid dissociation constant  $K_a$  and the local pH at the surface, the surface charge  $\sigma_{\text{surf}}$  associated with the surface groups is given by<sup>19</sup>

$$\sigma_{\text{surf}} = eN(1 + 10^{\text{pH}-\text{p}K_a} \exp(e\varphi/k_B T))^{-1}$$

where  $N$  is the total number of surface groups,  $e$  is the elementary charge,  $\varphi$  is the surface potential,  $k_B$  is the Boltzmann constant, and  $T$  is the temperature. Further details can be found in the Supporting Information. The diffuse countercharge in the electrolyte  $\sigma_{\text{dif}}$  is given by

$$\sigma_{\text{dif}} = \left( 2k_B T \varepsilon \varepsilon_0 \sum_i c_i^0 \left[ \exp\left(\frac{-ez_i \varphi}{k_B T}\right) - 1 \right] \right)^{1/2}$$

where  $\varepsilon$  is the dielectric constant of the electrolyte,  $\varepsilon_0$  is the vacuum permittivity, and  $c_i^0$  is the concentration and  $z_i$  is the valence of the ions  $i$  in the electrolyte. Assuming charge neutrality at the Dirac point, that is,  $\sigma_{\text{surf}} = \sigma_{\text{dif}}$ , these equations can be solved self-consistently. The result of this model is shown in Figure 2d (solid lines) using a surface group with  $\text{p}K_a = 4.5$  and a density of  $2 \times 10^{14}$  cm<sup>-2</sup> in the case of the nonfunctionalized, pristine graphene SGFETs. The exact nature

of these groups remains still unclear. We have investigated different substrates as well as a different copper etchant (see Supporting Information, Figure S3), but no conclusive results could be obtained. Possibly, OH defects on the graphene surface are responsible for this pH sensitivity as the  $\text{p}K_a$  of OH groups on several surfaces typically lies around 4.5.<sup>20,21</sup> The measured sensitivity is in good agreement with the values obtained for exfoliated and CVD grown graphene measured on various substrates.<sup>22,19,23</sup> However, another group observed a significantly lower sensitivity for high-quality CVD and exfoliated graphene, which could even be completely suppressed by a passivation of the surface.<sup>24</sup> This indicates that the sensitivity is related to defects and contaminations from the transfer. For epitaxial graphene, higher values were reported indicating a different mechanism for the pH sensitivity.<sup>25</sup>

Besides this lack in reliability, it can be seen from Figure 2d that the pH sensitivity of G-SGFETs at physiological pH is rather low (10 mV/pH), whereas the optimum operational pH of AChE lies between 7.5 and 8.<sup>26</sup> The reason for the low sensitivity at neutral pH is directly linked to the  $\text{p}K_a$  of the pH-sensitive surface groups. When the pH is sufficiently higher than the  $\text{p}K_a$ , all surface groups are already deprotonated and any further increase in pH cannot be detected by the transistor. For the unmodified transistor shown in Figure 2d, this range ends around pH 8. Therefore, unmodified G-SGFETs cannot provide a reliable pH sensitivity and do not offer a high sensitivity for the enzyme's activity in the relevant pH range. To overcome these problems, polymer brushes with DMAEMA groups were grown on the graphene transistors. The dimethyl amino groups of these polymers can be protonated with a reaction  $\text{p}K_a$  around 8,<sup>27</sup> thus enabling a high pH sensitivity in the pH range of interest. Figure 2d shows the pH response of a DMAEMA functionalized transistor, confirming an enhanced pH sensitivity starting around pH 6. Furthermore, the original sensitivity with an unclear origin is suppressed. From the fitting of the pH model to this data set, one can infer the presence of pH sensitive groups with a  $\text{p}K_a$  of 7.5 and a density of  $6 \times 10^{14}$  cm<sup>-2</sup>, assuming that the charged groups are located directly at the graphene's plane. Due to the high ionic strength of the electrolyte, which results in a Debye length smaller than 0.6 nm, only groups that are within this distance from the surface can contribute to signal. From our Raman data, it can be inferred that the defect density in the graphene is below  $3 \times 10^{11}$  cm<sup>-2</sup>.<sup>28</sup> As these defects are necessary for the grafting of the polymer brushes, the rather low density of polymer brushes along with the short Debye length cannot account for the high number of pH sensitive groups, in the hypothetical case that the polymers would be fully stretched. However, due to the high ionic concentration of the electrolyte and the absence of steric hindrance effects, the polymer brushes are expected to be in a collapsed configuration,<sup>29</sup> which can explain the high density of DMAEMA groups at the surface equivalent to a monolayer coverage.

After this basic characterization, transistors with DMAEMA and MAA copolymers were further functionalized with acetylcholinesterase via the formation of a peptide bond between the carboxylic group of the MAA and amino groups in the enzyme. The transistors were characterized to confirm that they are operational after the functionalization procedures (see Supporting Information, Figure S4 for the  $I$ – $V$  curves). Then, the response of the AChE-modified G-SGFETs to the neurotransmitter acetylcholine has been investigated. To this end, the transistors were biased at constant drain-source and

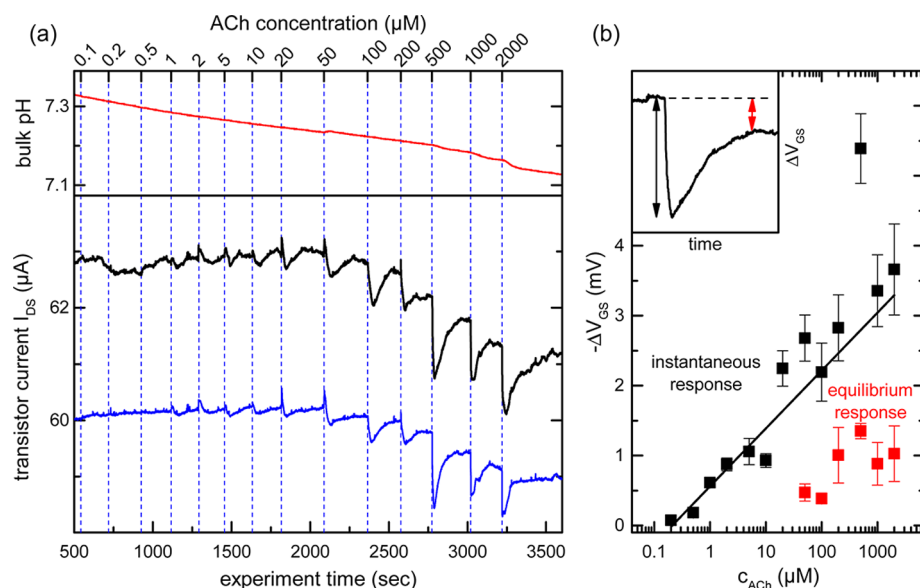


**Figure 3.** (a) Drain-source current of two transistors and pH of the bulk solution are shown versus time. At the marked times, acetylcholine was added to the solution, which can be seen in the transistor current as a sudden decrease. (b) Averaged instantaneous (black) and equilibrium (red) sensitivity to ACh for five transistors. The current change was converted to a change in the gate voltage  $V_{GS}$ . The line indicates a logarithmic fit of the instantaneous sensitivity. The inset shows how the instantaneous and equilibrium sensitivity are obtained.

gate-source voltages and the current was recorded continuously. At certain times, small amounts of an acetylcholine solution were added to the buffer to obtain previously calculated concentrations. Figure 3a shows an exemplary recording. The top scale marks the times at which acetylcholine was added to the buffer. A change in the current can be seen for ACh concentrations as low as  $0.5 \mu\text{M}$  and increases for higher concentrations. After the addition of the ACh, a fast decrease in the current can be observed followed by a slower increase which saturates below the original level (see inset in Figure 3b). The proton that is released during the enzyme activity lowers the local pH, which shifts  $V_D$  to more negative values. As the transistors were biased in the hole regime ( $V_{GS} < V_D$ ), this shift results in a lower current. The measured time dependence of the transistor response can be correlated with the fast kinetics of AChE: At very short times after the addition of ACh, all of the ACh molecules are quickly hydrolyzed by the enzymes resulting in a sudden increase in the proton concentration, given by the concentration of ACh. We will refer to this as instantaneous signal. Eventually, the overall reaction is dominated by diffusion, that is, ACh diffusing toward the transistor and proton diffusing away to the bulk solution. After some time, an equilibrium is reached with a proton concentration at the surface slightly higher than before. In Figure 3b, the averaged signal of five transistors is plotted versus the ACh concentration. To obtain comparable results, the transistor current is converted to an equivalent change in gate voltage by using the transistor transconductance.<sup>14</sup> For the instantaneous signal, a logarithmic sensitivity is obtained (Figure 3b). Considering that we can assume a proton concentration proportional to the ACh concentration for the instantaneous signal, the logarithmic dependence can be understood by recalling the linear response of the transistors to the pH (Figure 2d), that is, the logarithm of the proton concentration.

In summary, we have reported on a versatile platform for biosensing applications based on polymer-modified graphene FETs. The reported functionalization method of graphene

transistors with polymers allows the integration of several functionalities along surface-bound copolymer brushes without inducing damage to the graphene lattice. To demonstrate the capabilities of these multifunctional polymer brushes, we modified solution-gated graphene field-effect transistors with enzymes and transducing pH sensitive groups enabling the detection of the neurotransmitter acetylcholine. As the detection mechanism is based on the local pH change induced by the enzyme, our work can be extended to the detection of other biologically relevant analytes involved in enzymatic reactions resulting in the release of protons. In our experiments, we confirmed that the pH sensitivity can be controlled via the introduced pH sensitive groups in the polymer and that the activity of the enzyme acetylcholinesterase can be monitored with the functionalized transistor at acetylcholine concentrations as low as  $0.5 \mu\text{M}$ . Taking advantage of the transducing capability of graphene transistors and the versatility of polymer chemistry and enzyme biochemistry, this study presents a novel route for the fabrication of highly sensitive, multipurpose transistor sensors that can find application for a multitude of biologically relevant analytes.

## ■ ASSOCIATED CONTENT

### Supporting Information

Three additional figures and details on the employed pH model. This material is available free of charge via the Internet at <http://pubs.acs.org>.

## ■ AUTHOR INFORMATION

### Corresponding Author

\*E-mail: [garrido@wsi.tum.de](mailto:garrido@wsi.tum.de).

### Present Address

†F.D.: Consortium für elektrochemische Industrie, Wacker Chemie AG, Zielstattstraße 20, 81379 München, Germany.

### Notes

The authors declare no competing financial interest.

## ACKNOWLEDGMENTS

This work is funded by the German Research Foundation (DFG) in the framework of the Priority Program 1459 "Graphene", the European Union under the NeuroCare FP7 project (Grant Agreement 280433), and the Nanosystems Initiative Munich (NIM).

## REFERENCES

- (1) Novoselov, K. S. Electric Field Effect in Atomically Thin Carbon Films. *Science* **2004**, *306*, 666–669.
- (2) Schedin, F.; Geim, A. K.; Morozov, S. V.; Hill, E. W.; Blake, P.; Katsnelson, M. I.; Novoselov, K. S. Detection of Individual Gas Molecules Adsorbed on Graphene. *Nat. Mater.* **2007**, *6*, 652–655.
- (3) Allen, M. J.; Tung, V. C.; Kaner, R. B. Honeycomb Carbon: A Review of Graphene. *Chem. Rev.* **2010**, *110*, 132–145.
- (4) Cohen-Karni, T.; Qing, Q.; Li, Q.; Fang, Y.; Lieber, C. M. Graphene and Nanowire Transistors for Cellular Interfaces and Electrical Recording. *Nano Lett.* **2010**, *10*, 1098–1102.
- (5) Hess, L. H.; Jansen, M.; Maybeck, V.; Hauf, M. V.; Seifert, M.; Stutzmann, M.; Sharp, I. D.; Offenhäusser, A.; Garrido, J. A. Graphene Transistor Arrays for Recording Action Potentials from Electrogenic Cells. *Adv. Mater.* **2011**, *23*, 5045–5049.
- (6) Ohno, Y.; Maehashi, K.; Matsumoto, K. Label-Free Biosensors Based on Aptamer-Modified Graphene Field-Effect Transistors. *J. Am. Chem. Soc.* **2010**, *132*, 18012–18013.
- (7) Zeng, Q.; Cheng, J.; Tang, L.; Liu, X.; Liu, Y.; Li, J.; Jiang, J. Self-Assembled Graphene-Enzyme Hierarchical Nanostructures for Electrochemical Biosensing. *Adv. Funct. Mater.* **2010**, *20*, 3366–3372.
- (8) Shao, Y.; Wang, J.; Wu, H.; Liu, J.; Aksay, I. A.; Lin, Y. Graphene Based Electrochemical Sensors and Biosensors: A Review. *Electroanalysis* **2010**, *22*, 1027–1036.
- (9) He, R. X.; Lin, P.; Liu, Z. K.; Zhu, H. W.; Zhao, X. Z.; Chan, H. L. W.; Yan, F. Solution-Gated Graphene Field Effect Transistors Integrated in Microfluidic Systems and Used for Flow Velocity Detection. *Nano Lett.* **2012**, *12*, 1404–1409.
- (10) Niyogi, S.; Bekyarova, E.; Itkis, M. E.; Zhang, H.; Shepperd, K.; Hicks, J.; Sprinkle, M.; Berger, C.; Lau, C. N.; deHeer, W. A.; Conrad, E. H.; Haddon, R. C. Spectroscopy of Covalently Functionalized Graphene. *Nano Lett.* **2010**, *10*, 4061–4066.
- (11) Seifert, M.; Koch, A. H. R.; Deubel, F.; Simmet, T.; Hess, L. H.; Stutzmann, M.; Jordan, R.; Garrido, J. A.; Sharp, I. D. Functional Polymer Brushes on Hydrogenated Graphene. *Chem. Mater.* **2013**, *25*, 466–470.
- (12) Steenackers, M.; Gigler, A. M.; Zhang, N.; Deubel, F.; Seifert, M.; Hess, L. H.; Lim, C. H. Y. X.; Loh, K. P.; Garrido, J. A.; Jordan, R.; Stutzmann, M.; Sharp, I. D. Polymer Brushes on Graphene. *J. Am. Chem. Soc.* **2011**, *133*, 10490–10498.
- (13) Li, X.; Cai, W.; An, J.; Kim, S.; Nah, J.; Yang, D.; Piner, R.; Velamakanni, A.; Jung, I.; Tutuc, E.; Banerjee, S. K.; Colombo, L.; Ruoff, R. S. Large-Area Synthesis of High-Quality and Uniform Graphene Films on Copper Foils. *Science* **2009**, *324*, 1312–1314.
- (14) Hess, L. H.; Seifert, M.; Garrido, J. A. Graphene Transistors for Bioelectronics. *Proc. IEEE* **2013**, *101*, 1780–1792.
- (15) Hermanson, G. T. *Bioconjugate Techniques*; Academic Press: Amsterdam, 2008.
- (16) Steenackers, M.; Lud, S. Q.; Niedermeier, M.; Bruno, P.; Gruen, D. M.; Feulner, P.; Stutzmann, M.; Garrido, J. A.; Jordan, R. Structured Polymer Grafts on Diamond. *J. Am. Chem. Soc.* **2007**, *129*, 15655–15661.
- (17) Schoell, S. J.; Sachsenhauser, M.; Oliveros, A.; Howgate, J.; Stutzmann, M.; Brandt, M. S.; Frewin, C. L.; Sadow, S. E.; Sharp, I. D. Organic Functionalization of 3C-SiC Surfaces. *ACS Appl. Mater. Interfaces* **2013**, *5*, 1393–1399.
- (18) Dankerl, M.; Hauf, M. V.; Lippert, A.; Hess, L. H.; Birner, S.; Sharp, I. D.; Mahmood, A.; Mallet, P.; Veuillen, J.-Y.; Stutzmann, M.; Garrido, J. A. Graphene Solution-Gated Field-Effect Transistor Array for Sensing Applications. *Adv. Funct. Mater.* **2010**, *20*, 3117–3124.
- (19) Heller, I.; Chatoor, S.; Männik, J.; Zevenbergen, M. A. G.; Dekker, C.; Lemay, S. G. Influence of Electrolyte Composition on Liquid-Gated Carbon Nanotube and Graphene Transistors. *J. Am. Chem. Soc.* **2010**, *132*, 17149–17156.
- (20) Ong, S.; Zhao, X.; Eiseenthal, K. B. Polarization of Water Molecules at a Charged Interface: Second Harmonic Studies of the Silica/Water Interface. *Chem. Phys. Lett.* **1992**, *191*, 327–335.
- (21) Contescu, C.; Jagiello, J.; Schwarz, J. A. Heterogeneity of Proton Binding Sites at the Oxide/Solution Interface. *Langmuir* **1993**, *9* (7), 1754–1765.
- (22) Ohno, Y.; Maehashi, K.; Yamashiro, Y.; Matsumoto, K. Electrolyte-Gated Graphene Field-Effect Transistors for Detecting pH and Protein Adsorption. *Nano Lett.* **2009**, *9*, 3318–3322.
- (23) Maily-Giacchetti, B.; Hsu, A.; Wang, H.; Vinciguerra, V.; Pappalardo, F.; Occhipinti, L.; Guidetti, E.; Coffa, S.; Kong, J.; Palacios, T. pH Sensing Properties of Graphene Solution-Gated Field-Effect Transistors. *J. Appl. Phys.* **2013**, *114*, 84505.
- (24) Fu, W.; Nef, C.; Knopfmacher, O.; Tarasov, A.; Weiss, M.; Calame, M.; Schönenberger, C. Graphene Transistors are Insensitive to pH Changes in Solution. *Nano Lett.* **2011**, *11*, 3597–3600.
- (25) Ang, P. K.; Chen, W.; Wee, A. T. S.; Loh, K. P. Solution-Gated Epitaxial Graphene as pH Sensor. *J. Am. Chem. Soc.* **2008**, *130*, 14392–14393.
- (26) Silman, H. I.; Karlin, A. Effect of Local pH Changes Caused by Substrate Hydrolysis on the Activity of Membrane-Bound Acetylcholinesterase. *Proc. Natl. Acad. Sci. U.S.A.* **1967**, *58*, 1664.
- (27) van de Wetering, P.; Zuidam, N. J.; van Steenberg, M. J.; van der Houwen, O. A. G. J.; Underberg, W. J. M.; Hennink, W. E. A Mechanistic Study of the Hydrolytic Stability of Poly(2-(dimethylamino)ethyl methacrylate). *Macromolecules* **1998**, *31*, 8063–8068.
- (28) Cançado, L. G.; Jorio, A.; Martins Ferreira, E. H.; Stavale, F.; Achete, C. A.; Capaz, R. B.; Moutinho, M. V. O.; Lombardo, A.; Kulmala, T. S.; Ferrari, A. C. Quantifying Defects in Graphene via Raman Spectroscopy at Different Excitation Energies. *Nano Lett.* **2011**, *11*, 3190–3196.
- (29) Milner, S. T. Polymer Brushes. *Science* **1991**, *251*, 905–914.